Evidence for the Origin of Reconstruction of the Mo(001) Surface

J. W. Chung, K. S. Shin, D. H. Baek, C. Y. Kim, and H. W. Kim
Physics Department and the Basic Science Research Center, Pohang Institute of Science and Technology, Pohang, 790-330, Korea

S. K. Lee and C. Y. Park
Physics Department, Sungkyunkwan University, Suwon 440-746, Korea

S. C. Hong
Physics Department, University of Ulsan, Ulsan 680-749, Korea

T. Kinoshita, M. Watanabe, A. Kakizaki, and T. Ishii
Institute for Solid State Physics, The University of Tokyo, Roppongi, Minato-Ku, Tokyo 106, Japan
(Received 4 June 1992)

We report results of an angle-resolved photoemission study to elucidate the driving mechanism of the Mo(001) surface reconstruction. We find, for the first time, a remarkable change of the shapes of Fermi contours upon cooling, which reveals a significant nesting at $k_{\parallel}=0.65$ Å^{-1}, extended 0.30 Å^{-1} perpendicular to the $\bar{\Sigma}$ axis. The results suggest that the reconstruction should occur essentially by Peierls-type $2k_F$ instabilities with significant matrix element effects.

PACS numbers: 64.60.−i, 63.20.Kr, 73.20.At

A vast library for characteristic features of the reconstructional phase transitions of clean W(001) and Mo(001) surfaces has been established to date [1–21]. However, the physical origin that drives the reconstructions, which reveal distinctly different phases below transition temperatures (T_c) despite the isoelectronic nature of the surfaces, has not been completely resolved, especially for the Mo(001) surface. A clean Mo(001) surface undergoes a reconstructional phase transition from a (1×1) to an incommensurate $c(2.2\times2.2)$ phase upon cooling below $T_c=230$ K [1,2]. Recent ion-scattering and low-energy-electron-diffraction (LEED) studies suggest that the low-temperature phase is a commensurate $c(7\sqrt{2}\times\sqrt{2})$ phase, showing the subtlety of this phase [3,4].

Essentially two branches of theoretical models have been competing for this subject. A charge-density-wave (CDW) mechanism ascribes the reconstructions to the Peierls-like surface phonon instabilities driven by nesting of two-dimensional Fermi surfaces with the onset of a periodic lattice distortion [1,5–8]. On the other hand, a model based on the dynamic Jahn-Teller-like instabilities invokes a local bonding of surface orbitals that plays the role of impurity stabilizer for an intrinsically unstable surface [9–13]. Here a strong electron-lattice coupling stabilizes the surface by softening a mode of surface phonons at T_c. Thus in the CDW model electronic entropy governed by a temperature-dependent susceptibility that goes singular at T_c drives the transition. However, in the local-bonding model, phononic entropy from a temperature-dependent phonon frequency that softens at T_c is responsible for the reconstruction. Relatively few experimental efforts [6,13] have been made to examine the tenability of the theoretical models.

The purpose of this Letter is to present the results of an angle-resolved photoemission study, which provide new experimental evidence for the driving mechanism of Mo(001) reconstruction. We measured the temperature dependence of Fermi-surface contours to reveal a significant nesting effect at T_c, supporting essentially the CDW model with nontrivial matrix element effects.

The experiment was performed using synchrotron uv radiation on the ISSP (Institute for Solid State Physics) beam line BL-18A at the Photon Factory in Japan. Typical energy and angular resolutions are less than 150 meV and 1°. The sample surface, oriented within ±0.2° to a (001) plane, was cleaned by a well-known recipe [1], and produced the incommensurate $c(2.2\times2.2)$ LEED pattern at low temperature. A quartet of extra spots near $\bar{M}=(\pi/a)(1,1)=1.4$ Å^{-1} in the surface Brillouin zone (SBZ) stayed strong and sharp for at least 20 min, and still discernible after 40 min under a base pressure of below 2×10^{-11} Torr. We were not able to observe the $(7\sqrt{2}\times\sqrt{2})$ LEED pattern for temperatures down to 52 K, in contradiction to a recent study [3]. In order to vary the sample temperature in the range of 50 to 2500 K, we used a closed-cycle cold head thermally connected to the sample, and electron-beam-bombardment heating.

Since we observe several new features in the surface band dispersions not available in calculations to date [14,15], we also have carried out band calculations using the full-potential linearized augmented plane-wave (FLAPW) method for a seven-layer slab for a bulk-truncated (1×1) surface. The results qualitatively reproduce the main features of the experimental observations, and unveil symmetries of the states. Since the details of the band dispersions, both theory and experiment, will be reported elsewhere [16], we focus here on mapping

Fermi-surface contours from these spectra to elucidate the driving mechanism of the reconstruction.

A series of photoemission spectra with two-dimensional wave vectors $k_\parallel$ along the $\bar{\Sigma}$ axis are presented in Fig. 1 for a reconstructed surface at $T=52$ K. The data were obtained with photons of energy 21.22 eV, incident at 45° to the surface normal with photon polarization in a (110) scattering plane. Corresponding spectra for an unreconstructed surface for $T \geq T_c$, not shown here, are basically similar to those in Fig. 1, and qualitatively agree with previous studies [13,17]. In Fig. 1, in order to emphasize the details, we intentionally present many spectra separated by $\Delta k_\parallel = 0.037$ Å^{-1} from each other. The normal emission ($k_\parallel = 0$, $\bar{\Gamma}$) in Fig. 1 shows two predominant peaks: a so-called Swanson hump state S_1 of a nearly flat band of binding energy E (< -0.2 eV) just below the Fermi energy E_F, and a strong bulk peak B_1 of $E = -1.3$ eV. A weak surface resonance SR_1 of $E \cong -0.6$ eV grows in intensity, and mixes with S_1 with $k_\parallel$. We find that B_1 becomes another surface resonance SR_2 for $k_\parallel \geq 0.51$ Å^{-1}. These classifications of the peaks were made by examining the surface nature of the peaks experimentally through a method well known in the literature [13], and comparing to the results of our theoretical calculation as discussed below.

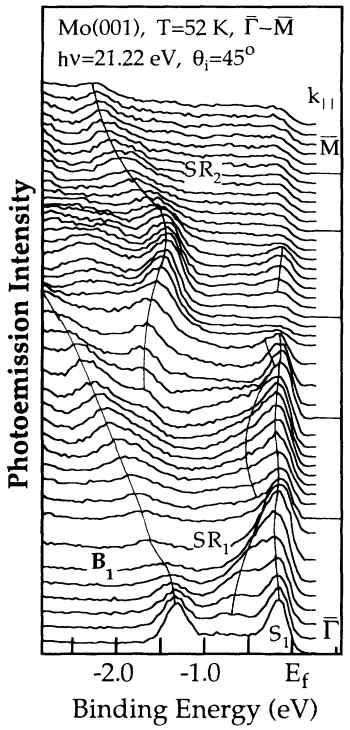

FIG. 1. A series of angle-resolved photoemission spectra with $k_\parallel$ along the $\bar{\Sigma}$ axis with a sample at $T=52$ K (below T_c). The spectra were separated by about 0.037 Å^{-1}, starting from $\bar{\Gamma}$ ($k_\parallel = 0$ Å^{-1}, bottom) to $\bar{M}$ ($k_\parallel = 1.4$ Å^{-1}, sixth from the top). The spectra with extended ends beyond E_F have $k_\parallel = 0.29$, 0.61, 0.89, 1.21, and 1.42 Å^{-1}, respectively from the bottom.

As noted earlier [13,17], S_1 is found to be extremely sensitive to surface contamination, especially to hydrogen atoms, and does not disperse with incident photon energy, as for a true surface state. A surface state similar to S_1 was also found on a W(001) surface [18], and the origin of these intense surface states has been a subject of a number of theoretical studies [8,14–16]. The states SR_1 and SR_2 are much less sensitive to surface contaminations compared to S_1 and somewhat dispersive with photon energy. Our calculation reveals, however, that more than 50% of their charges reside on the surface, typical for a resonance state.

Two-dimensional Fermi-surface contours were measured by determining the Fermi wave vectors $k_\parallel^F$ at which S_1 crosses E_F for the entire area of the $\frac{1}{8}$ irreducible SBZ. As discussed previously [13,19], an exact location of $k_\parallel^F$ is normally complicated by experimental restrictions such as a finite energy resolution. Since the main goal of the present study is to probe the shape of the Fermi contours, we determine $k_\parallel^F$ systematically so that the shape may remain unaffected although the area covered by the contours may vary upon choosing different Fermi vectors.

While S_1 shows a small dispersion ($E \leq -0.3$ eV) for $k_\parallel \leq 0.78$ Å^{-1} where it disappears completely, SR_1 displays a significant variation of binding energy in a periodic fashion. Initially it approaches E_F up to about $k_\parallel = 0.2$ Å^{-1}, and then disperses away until about $k_\parallel = 0.47$ Å^{-1} for the maximum binding energy of -0.64 eV. As $k_\parallel$ increases further, SR_1 reapproaches E_F up to $k_\parallel = 0.70$ Å^{-1}, where it again disperses away while the intensity decreases rapidly at the same time. These behaviors are clearly seen in the dispersions in Fig. 2, with our calculated surface bands also drawn as solid curves.

We find both theoretically and experimentally that S_1

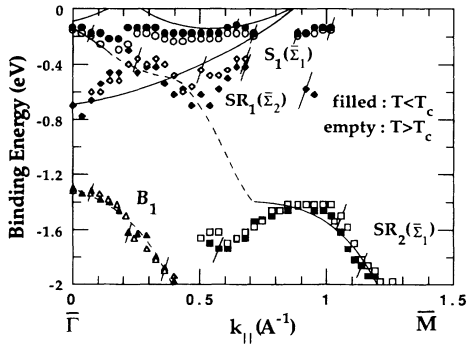

FIG. 2. Experimental (symbols) and theoretical (solid curves) band dispersions of Mo(001) surface. Surface state S_1, surface resonances SR_1 and SR_2, and bulk state B_1 are denoted by circles, diamonds, squares, and triangles, respectively, with even ($\bar{\Sigma}_1$) and odd ($\bar{\Sigma}_2$) symmetries specified. The solid and open symbols are for below and above T_c, and solid (dashed) curves are our theoretical curves for surface (bulk) states. Representative error bars are drawn as short slanted lines.

is mainly of even ($\bar{\Sigma}_1$) and SR_1 is of odd ($\bar{\Sigma}_2$) character except near $\bar{\Gamma}$ where S_1 mixes with states of odd symmetry in a limited range of $k_\parallel$. We note that the calculated bands of S_1 and SR_1 disappear at $k_\parallel = 0.88$ Å^{-1} simultaneously, in qualitative agreement with experiment. Interestingly there appears a band of weak intensity for a narrow region of $0.87 < k_\parallel < 1.06$ Å^{-1}, absent in the calculated surface bands. Although not shown in Fig. 2, this band, another surface resonance, stems from a bulk band that crosses E_F near $\bar{M}$ [16]. A big hole pocket centered at $\bar{M}$ begins at $k_\parallel = 1.06$ Å^{-1} where this weak resonance state dies out as observed previously [13].

In Fig. 3, we plot the two-dimensional Fermi-surface contours C_F for the $\frac{1}{4}$ SBZ for above (a) and below (b) T_c, which reveal an important aspect for the origin of the reconstruction. The complete contours were made by mirror reflecting the data obtained for the $\frac{1}{8}$ irreducible SBZ. As mentioned earlier, bearing the experimental limitations in mind, the contours C_0 were determined by $k_\parallel$ values where S_1 disappears completely, and then the Fermi contours C_F by the wave vectors where S_1 approaches closest to E_F within the experimental resolution of 0.15 eV. The Fermi vector $k_\parallel^F$ thus chosen along $\bar{\Sigma}$ is

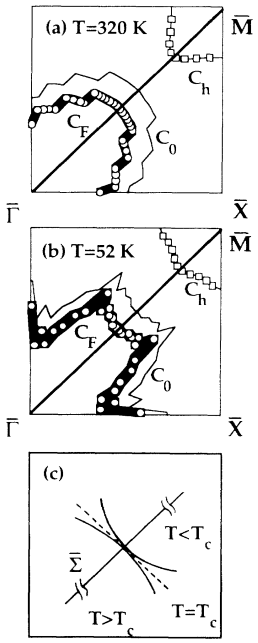

FIG. 3. (a) Experimentally determined Fermi-surface contours for the $\frac{1}{4}$ surface Brillouin zone ($T > T_c$). (b) Corresponding contours at $T < T_c$. The contours are defined by wave vectors where S_1 approaches closest to E_F (C_F), disappears completely (C_0), and disappears again (C_h). The shaded areas denote the error range of the contours. (c) The segments of C_F along the direction perpendicular to the $\bar{\Sigma}$ axis are redrawn to emphasize the change of the curvature, from convex to concave, upon cooling below T_c. A perfect nesting should occur exactly at T_c that can extend about 0.30 Å^{-1}, which might be enough to induce reconstruction via the CDW mechanism.

0.65 Å^{-1} (see Fig. 2), which deviates from the theoretical E_F crossing of 0.88 Å^{-1}. It is also not unique in the sense that there exists a range $0.21 \leq k_\parallel \leq 0.36$ Å^{-1} where S_1 also approaches close to E_F within the energy resolution. A big hole pocket C_h centered at $\bar{M}$ and surrounded by a weak electron pocket (not shown to avoid complication in the figures) is found, in agreement with previous measurement [13].

The temperature dependence of the Fermi contours in Fig. 3, reported for the first time, shows a remarkable change of their shapes upon cooling. In Fig. 3(c), the segments of Fermi contours perpendicular to the $\bar{\Sigma}$ axis are redrawn schematically to emphasize the change of the curvature, from convex to concave as temperature crosses T_c, which suggests a good possibility of a perfectly parallel segment exactly at T_c. The length of the parallel segment at T_c is estimated to be about 0.30 Å^{-1}, which should be enough to enhance the generalized susceptibility to soften, with nonadiabatic effects, a surface mode as in the CDW model [9]. Thus the $2k_F$ instability of the Peierls type plays a vital role for the reconstruction, and naturally accounts for the wave vector of reconstruction $2k_\parallel^F = 1.30$ Å^{-1}, in close agreement with the LEED observation of $q_\parallel = 1.28$ Å^{-1} in the $c(2.2\times2.2)$ phase. As discussed by Smith and Kevan, a symmetry argument selects the M_5 mode to be pinned at T_c [13].

It is also instructive to choose $k_\parallel^F = 0.78$ Å^{-1} where both S_1 and SR_1 disappear. We then have an even more significant nesting effect that might freeze the M_5 mode of $q_\parallel = G - 2k_\parallel^F = 1.24$ Å^{-1}. We further find that there are no such parallel segments perpendicular to $\bar{\Sigma}$ for an electron pocket surrounding the hole pocket at $\bar{M}$ or for the hole pocket itself.

In contrast, we now consider several features that might support the local bonding mechanism. The fact that there exists a strong surface state of flat band near E_F, which mixes with a surface resonance periodically, suggests a significant nonadiabatic electron-lattice cou-

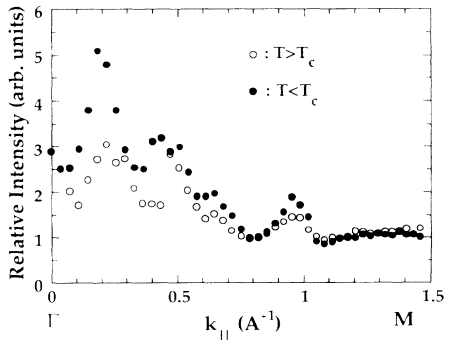

FIG. 4. Ratio of the peak intensity of S_1 normalized by a background intensity, taken at binding energy -1.0 eV. Solid and open circles are for below and above T_c. Notice the periodic variation with periodicity of about 0.21 Å^{-1}, and enhanced intensity at low temperature.

pling as in the local bonding model [9]. Moreover, the peak intensity of S_1, being proportional to the surface density of states, also shows an interesting oscillatory behavior as depicted in Fig. 4 for above (open circles) and below (solid circles) T_c. The intensity was normalized by a background intensity, taken at $E \cong -1.0$ eV, where the intensity variation with $k_\parallel$ remains minimal. Note the periodicity of about $k_\parallel = 0.21$ Å^{-1} for both temperatures, which is half of that of the $(7\sqrt{2}\times\sqrt{2})$ phase. We also observe much enhanced intensity, especially at $k_\parallel = 0.21$ Å^{-1}, at low temperature, and the low intensity at $k_\parallel^f$ demands nontrivial matrix element effects in addition to Fermi-surface nesting. Similar distributions of the surface density of states were found for the region nearby the $\bar{\Sigma}$ axis in the SBZ.

If the local bonding mechanism works solely for the reconstruction, there should be a strong matrix element effect, winning the distribution of surface states in Fig. 4, in selecting the wave vector of the reconstruction $q_\parallel = 0.40$ or 1.28 Å^{-1} for the $(7\sqrt{2}\times\sqrt{2})$ [3,4] or the $c(2.2\times2.2)$ phase [1]. However, this is not consistent with recent observations [20,21] that a significant Kohn anomaly in the M_5 phonon mode occurs only at $q = 1.1$ Å^{-1} above T_c along $\bar{\Sigma}$, while other phonon modes are forbidden by the symmetry selection rule [13]. It is worth noting the possibility that the strong periodic modulation of the surface resonance SR_1 might be caused by the reconstruction penetrating into subsurface layers, an indication of involvement of phonons with vertical displacements as noted previously [3,22].

In summary, we measured the temperature dependence of two-dimensional Fermi-surface contours of a clean Mo(001) surface and show that a significant nesting occurs at T_c with Fermi vector that accounts for the wave vector of the reconstruction. The surface density of states at the Fermi vector, however, is found to be a local maximum. We thus conclude that the reconstruction should occur essentially via the CDW mechanism with considerable matrix element effects.

This work was supported in part by the user program of Pohang Light Source and the Ministry of Education, Korea, through Basic Science Research Center.

[1] T. E. Felter, R. A. Barker, and P. J. Estrup, Phys. Rev. Lett. **38**, 1138 (1977).
[2] M. K. Debe and D. A. King, Phys. Rev. Lett. **39**, 708 (1977).
[3] M. L. Hildner, R. S. Daley, T. E. Felter, and P. J. Estrup, J. Vac. Sci. Technol. A **9**, 1604 (1991).
[4] D.-M. Smilgies and E. Hulpke, Phys. Rev. B **43**, 1260 (1991).
[5] E. Tossatti, Solid State Commun. **25**, 637 (1978).
[6] J. C. Campuzano, D. A. King, C. Somerton, and J. E. Inglesfield, Phys. Rev. Lett. **45**, 1649 (1980).
[7] J. E. Inglesfield, J. Phys. C **11**, L69 (1978).
[8] H. Krakauer, M. Posternak, and A. J. Freeman, Phys. Rev. Lett. **43**, 1885 (1979).
[9] J. E. Inglesfield, J. Phys. C **12**, 149 (1979).
[10] K. Terakura, I. Terakura, and Y. Teraoka, Surf. Sci. **86**, 535 (1979).
[11] J. C. Campuzano, J. E. Inglesfield, D. A. King, and C. Somerton, J. Phys. C **14**, 3099 (1981).
[12] D. Singe and H. Krakauer, Phys. Rev. B **37**, 3999 (1988).
[13] Kevin E. Smith and Stephen D. Kevan, Phys. Rev. B **43**, 3986 (1991).
[14] C. M. Bertoni, C. Calandra, and F. Manghi, Solid State Commun. **23**, 255 (1977).
[15] P. C. Stephenson and D. W. Bullett, Surf. Sci. **139**, 1 (1984), and references therein.
[16] K. S. Shin, J. W. Chung, C. Y. Park, S. C. Hong, T. Kinoshida, M. Watanabe, A. Kakizaki, and T. Ishi (to be published).
[17] Shang-Lin Weng, T. Gustafsson, and E. W. Plummer, Phys. Rev. Lett. **39**, 822 (1977).
[18] Kevin E. Smith, Greg S. Elliot, and Stephen D. Kevan, Phys. Rev. B **42**, 5385 (1990).
[19] R. Clauberg, K. H. Frank, J. M. Nicholls, and B. Reihl, Surf. Sci. **189/190**, 44 (1987).
[20] E. Hulpke and D.-M. Smilgies, Phys. Rev. B **40**, 1338 (1989).
[21] X. W. Wang, C. T. Chan, K. M. Ho, and W. Weber, Phys. Rev. Lett. **60**, 2066 (1988).
[22] C. Z. Wang, A. Fasolino, and E. Tosatti, Surf. Sci. **212**, 323 (1989).